

Spatial structure of anomalously localized states in disordered conductors

V. Uski and B. Mehlig

Physics and Engineering Physics, Gothenburg University/Chalmers, SE-41296 Gothenburg, Sweden

M. Schreiber*

School of Engineering and Science, International University Bremen, D-28725 Bremen, Germany

(Received 10 June 2002; published 13 December 2002)

We study the spatial structure of wave functions with exceptionally high local amplitudes in the Anderson model of localization. By means of exact diagonalizations of finite systems, we obtain and analyze images of these wave functions: we compare the spatial structure of such anomalously localized states in quasi-one-dimensional samples to that in three-dimensional samples. In both cases the average wave-function intensity exhibits a very narrow peak. The background intensity, however, is found to be very different in these two cases: in three dimensions, it is constant, independent of the distance to the localization center (as expected for extended states). In quasi-one-dimensional samples, on the other hand, it is redistributed towards the localization center and approaches a characteristic form predicted by Mirlin [Phys. Rep. **326**, 249 (2000)].

DOI: 10.1103/PhysRevB.66.233104

PACS number(s): 72.15.Rn, 71.23.An, 05.40.-a

Statistical properties of physical observables in disordered electronic quantum systems have attracted considerable interest in the last decade. In such systems, quantum interference may cause the (noninteracting) conduction electrons to localize.¹ In three dimensions, this Anderson localization occurs when the disorder strength exceeds a critical value. Beyond this value (which depends on the Fermi energy and the symmetries of the system), electron wave functions are confined to a limited spatial region of the sample.

In the metallic regime, in contrast, wave functions typically spread over the whole sample, and they contribute to electron transport. However, some wave functions show localized behavior even in this weakly disordered regime [so-called anomalously localized states, (ALS's)]. This leads to a nonzero, albeit small, probability of observing exceptionally large wave-function amplitudes (*rare events*), often in the form of a log-normal distribution function of amplitudes. ALS's in electronic conductors have been studied intensively in recent years, using the so-called diffusive nonlinear σ model (DNLSM).²⁻⁴ An overview of the main results and predictions based on the DNLSM is given in Ref. 6. Moreover, possible complications due to nondiffusive, so-called ballistic effects on length scales smaller than the mean free path are discussed. As was pointed out in Ref. 8, these may modify the predictions of the DNLSM (see also Refs. 9 and 10). ALS's are expected to occur in lower-dimensional disordered systems, too, when the disorder is weak.

These interesting analytical results have motivated a number of numerical studies: in Ref. 7, for example, log-normal statistics of wave-function amplitudes in two-dimensional (2D) conductors near the delocalization-localization transition was observed. In Ref. 11 it was confirmed that as the disorder is reduced to reach the weakly disordered regime, the distribution function remains log-normal. It has, however, not been possible to resolve a discrepancy (between the DNLSM^{5,6} and the so-called direct optimal fluctuation method⁸) in the prediction of the parameters of this distribution. As far as the numerical work is concerned, the situation

may be summarized as follows. While it can be concluded that the DNLSM appears to be adequate in the quasi-one-dimensional (Q1D) Anderson model under certain conditions,^{11,10} the DNLSM may not correctly describe ALS's in two and three dimensions,^{10,12} at least for the parameter values considered in these studies. On the other hand, it was found recently¹⁴ that the DNLSM appears to describe the statistics of rare events adequately in a 2D kicked rotor.

A reason for the possible failure of the DNLSM to describe ALS's in the three-dimensional (3D) Anderson model may be the importance of short length scales,^{8,9} (see also Ref. 10). The DNLSM is based on the semiclassical picture of a diffusing electron in a random potential. In this picture the smallest relevant length scale is the electronic mean free path l between elastic collisions. Therefore the DNLSM cannot describe situations where length scales smaller than l are important. Such a situation could occur if ALS's were created not through semiclassical diffusion, but through local potential wells trapping the electrons.^{8,15} The mechanism giving rise to ALS's is expected^{6,8,16} to crucially depend on the dimensionality of the system and may determine their spatial structure.

Finally, within the DNLSM, it is possible to obtain the wave-function statistics directly in Q1D, using a transfer-matrix technique. In two and three dimensions, on the other hand, a further saddle-point approximation is necessary. Given this situation, further numerical work describing ALS's in disordered conductors is called for. In the following, we describe results of exact diagonalizations of finite Anderson models of localization, yielding averages of the *spatial structure* of ALS's. While this spatial structure has been studied in detail within the DNLSM,^{6,16} numerical imaging of wave functions with anomalously amplitudes has not yet been performed.¹³

The Anderson model is defined by the tight-binding Hamiltonian

$$\hat{H} = \sum_{\mathbf{r}, \mathbf{r}'} t_{\mathbf{r}\mathbf{r}'} c_{\mathbf{r}}^\dagger c_{\mathbf{r}'} + \sum_{\mathbf{r}} v_{\mathbf{r}} c_{\mathbf{r}}^\dagger c_{\mathbf{r}} \quad (1)$$

on a hypercubic lattice. Here $c_{\mathbf{r}}^\dagger$ and $c_{\mathbf{r}}$ are the creation and annihilation operators at site \mathbf{r} , the hopping amplitudes are $|t_{\mathbf{r}\mathbf{r}'}| = 1$ for nearest-neighbor sites and zero otherwise. The on-site potentials $v_{\mathbf{r}}$ are Gaussian distributed with zero mean and $\langle v_{\mathbf{r}} v_{\mathbf{r}'} \rangle = (W^2/12) \delta_{\mathbf{r}\mathbf{r}'}$. As usual, the parameter W characterizes the strength of the disorder and $\langle \dots \rangle$ denotes the disorder average. We study finite Q1D and 3D lattices.

It has been suggested in Ref. 3 to characterize the spatial structure of ALS's by means of conditional averages of the form $\langle V^q |\psi(\mathbf{r})|^{2q} \rangle_t$. Here $\langle \dots \rangle_t$ denotes an average over all wave functions with $t = V |\psi(\mathbf{0})|^2$, $q = 1, 2, \dots$, and V is the volume of the system [wave functions are normalized so that $\langle |\psi_j(\mathbf{r})|^2 \rangle = V^{-1}$]. For large values of t , the average $\langle V^q |\psi(\mathbf{r})|^{2q} \rangle_t$ describes how wave functions decay, on average, away from the localization center.

In the metallic regime, typical wave functions fluctuate as described by random matrix theory^{17,18} (RMT). Depending on the symmetries of Eq. (1), Dyson's Gaussian orthogonal or unitary ensembles are appropriate.¹⁸ We refer to these two cases by assigning, as usual, the parameter $\beta=1$ to the former and $\beta=2$ to the latter. Within RMT, for $\mathbf{r} \neq 0$,

$$\langle V^q |\psi(\mathbf{r})|^{2q} \rangle_t = \begin{cases} 1 & \text{if } q=1, \\ 3 & \text{if } q=2 \text{ and } \beta=1, \\ 2 & \text{if } q=2 \text{ and } \beta=2. \end{cases} \quad (2)$$

This reflects the fact that in a metallic system, wave functions spread uniformly over the whole sample with spatially short-ranged correlations.^{3,9} In the presence of ALS's, the conditional averages $\langle V^q |\psi(\mathbf{r})|^{2q} \rangle_t$ are expected to differ from Eq. (2).

In order to characterize the spatial structure of ALS's in the weakly disordered Anderson model, the conditional averages $\langle \dots \rangle_t$ were calculated within the DNLSM in Refs. 3 and 16. For $q=1$ the authors write

$$\langle V |\psi(\mathbf{r})|^2 \rangle_t = g(E, t; \mathbf{r}) / f(E, t), \quad (3)$$

where $f(E, t)$ is defined as

$$f(E, t) = \Delta \left\langle \sum_j \delta(t - V |\psi_j(\mathbf{0})|^2) \right\rangle_{E_j=E}. \quad (4)$$

Here Δ is the mean energy level spacing and $\langle \dots \rangle$ denotes a combined disorder and energy average (over a small interval of width η centered around E). The function $g(E, t; \mathbf{r})$ is defined as

$$g(E, t; \mathbf{r}) = \Delta \left\langle \sum_j V |\psi_j(\mathbf{r})|^2 \delta(t - V |\psi_j(\mathbf{0})|^2) \right\rangle_{E_j=E}. \quad (5)$$

Below, we take the δ -functions in Eqs. (4) and (5) to be slightly broadened with small but finite width $\gamma > 0$.

In close vicinity of the localization center, ALS's are found to exhibit a very narrow peak (of width less than l). The expressions below apply for $r > l$ and thus describe the

smooth background intensity, but not the sharp peak itself.¹⁶ For $\beta=2$ one obtains for a Q1D conductor^{3,16}

$$f(E, t) = \frac{d^2}{dt^2} [\mathcal{W}^{(1)}(t/X, \tau_+) \mathcal{W}^{(1)}(t/X, \tau_-)] \quad (6)$$

and (assuming $|\mathbf{r}| \equiv r > l$)

$$g(E, t; \mathbf{r}) = -X \frac{d}{dt} \left[\frac{\mathcal{W}^{(2)}(t/X, \tau_1, \tau_2) \mathcal{W}^{(1)}(t/X, \tau_-)}{t} \right], \quad (7)$$

where $\tau_+ = (L-x)/\xi$, $\tau_- = x/\xi$, $\tau_1 = r/\xi$, and $\tau_2 = (L-x-r)/\xi$. Here, $X = L/\xi$, L is the length of the sample, and ξ is the localization length. Moreover, x is the distance of the observation point from the edge of the sample (cf. Refs. 3 and 16). The function $\mathcal{W}^{(1)}(z, \tau)$ obeys the differential equation

$$\frac{\partial}{\partial \tau} \mathcal{W}^{(1)}(z, \tau) = \left(z^2 \frac{\partial^2}{\partial z^2} - z \right) \mathcal{W}^{(1)}(z, \tau) \quad (8)$$

with initial condition $\mathcal{W}^{(1)}(z, 0) = 1$. The function $\mathcal{W}^{(2)}(z, \tau, \tau')$ obeys the same differential equation, but with the initial condition $\mathcal{W}^{(2)}(z, 0, \tau) = z \mathcal{W}^{(1)}(z, \tau)$.

For large values of t , it is suggested in Ref. 16 that the background intensity should be given by

$$\langle V |\psi(\mathbf{r})|^2 \rangle_t \approx \frac{1}{2} \sqrt{tX} [1 + r \sqrt{t/(L\xi)}]^{-2}, \quad (9)$$

where in accordance with the above $r > l$ is assumed, and also $r \ll \xi$. Corresponding expressions may be obtained for higher values of q . One expects¹⁶ (for $l < r \ll \xi$)

$$\langle V^q |\psi(\mathbf{r})|^{2q} \rangle_t \approx q! [\langle V |\psi(\mathbf{r})|^2 \rangle_t]^q. \quad (10)$$

In three-dimensions, by contrast, results corresponding to Eqs. (8)–(10) are not known,¹⁶ but it is expected that the background intensity of ALS's is characteristically different from that in Q1D samples: ALS's in 3D systems are expected^{8,6} to exhibit a very narrow maximum near the localization center (the width of this peak is a matter of current debate^{8,6}). The background, however, is expected^{16,6} to decay very quickly to $\langle V |\psi(\mathbf{r})|^2 \rangle_t \approx 1$. Furthermore, fluctuations around this average are expected¹⁶ to be described by RMT [see Eq. (2)].

In the following we describe and discuss results of exact-diagonalizations¹⁹ of the Anderson Hamiltonian (1) and compare to the results of the previous section. We emphasise that at least in three dimensions it is important to use a Gaussian distribution for the on-site potentials in order to be able to compare to the analytical predictions: ALS's are possibly *non-universal*, their spatial structure may depend on the properties of the random potential.

Our numerical results for $\langle V |\psi(\mathbf{r})|^2 \rangle_t$ and $\langle V^2 |\psi(\mathbf{r})|^4 \rangle_t$ are summarized in Figs. 1–4. Figures 1 and 3 show results for Q1D samples with $\beta=2$, while Figs. 2 and 4 show results for 3D samples and $\beta=1$.

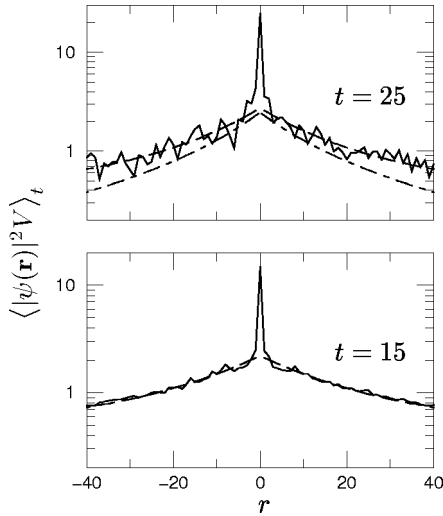


FIG. 1. Spatial structure of anomalously localized wave functions with $t=|\psi(0)|^2V$. Solid lines: Numerical results for $V=128 \times 4 \times 4$ (Q1D case), disorder $W=1.6$, and energy $E \approx -1.7$, averaged over 40 000 wave functions. Dashed lines: Analytical predictions with $X=0.97$ [full formula (Ref. 21), with Eqs. (6) and (7)]. The dash-dotted line shows the asymptotic formula, Eq. (9), for $t=25$.

In all cases we see a very narrow peak at the localization center. Our main results, however, concern characteristic differences between the distribution of background intensities in Q1D and 3D samples. In the Q1D case we observe a global redistribution of background intensity towards the localization center (as compared with uniformly spread RMT wave functions). The numerical results are very well described by Eqs. (6)–(8). The asymptotic formula (9) considerably underestimates $\langle V|\psi(\mathbf{r})|^2 \rangle_t$ for the values of t used in Fig. 1. In the 3D case, by contrast, the background intensity is roughly constant (Fig. 2). This is consistent with the qualitative picture summarized above.

Figures 3 and 4 show the second moments, i.e., the case $q=2$. In Q1D samples, Eq. (10) appears to be valid for large

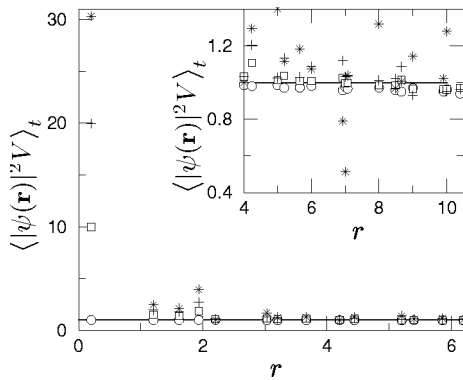


FIG. 2. Spatial structure of anomalously localized wave functions with $t=|\psi(0)|^2V$. Numerical results for $V=48 \times 48 \times 48$ (3D case), disorder strength $W=2$, and energy $E \approx -1.7$, averaged over 88 wave functions. The symbols show the numerically calculated values for $t=1$ (\circ), $t=10$ (\square), $t=20$ ($+$), and $t=30$ ($*$). The line shows the constant RMT average intensity $\langle |\psi(\mathbf{r})|^2 V \rangle_t = 1$.

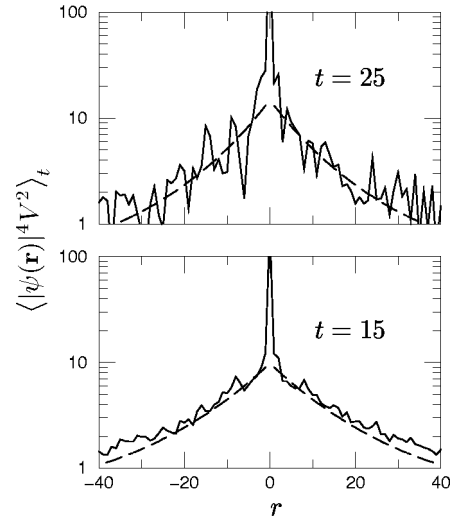


FIG. 3. Solid lines: The function $\langle V^2|\psi(r)|^4 \rangle_t$ in the Q1D case averaged over the same wave functions as in Fig. 1. The dashed lines show the function $2[\langle V|\psi(r)|^2 \rangle_t]^2$, where $\langle V|\psi(r)|^2 \rangle_t$ is calculated from Eqs. (8)–(10).

t , as expected. In 3D samples, the fluctuations of the background intensity appear to be consistent with the RMT statistics (although the scatter is large). That is, they are roughly constant as a function of r , as predicted in Ref. 16. However, a closer inspection shows (inset of Fig. 4) that the second moment is somewhat higher than expected according to RMT. This is possibly due to the finite conductance in the system.^{3,16} The dip at $r \sim 7$ with $t=30$ could be due to insufficient averaging. Our current data do not permit to draw a definite conclusion here, it could also represent a systematic effect.

Summarizing our results for $r > l$, we have made the following observations. First, in our simulations, the spatial structure of ALS's depends on the dimension. In Q1D samples, we have observed a global redistribution of the background intensity towards the localization center (as compared with typical, uniformly spread extended states). In 3D samples, on the other hand, the background intensity is roughly constant; the wave-function intensity is significantly

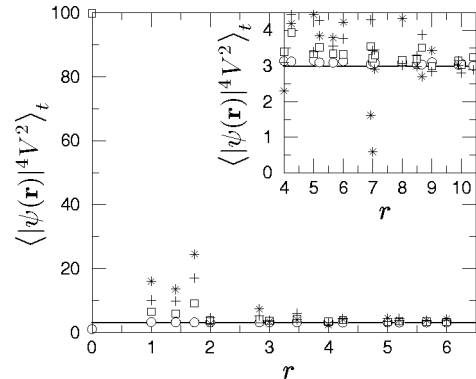


FIG. 4. The function $\langle V^2|\psi(r)|^4 \rangle_t$ in the 3D case. The symbols show the numerically calculated values. The parameters and symbols are the same as in Fig. 2. The line shows the constant RMT fluctuations, $\langle V^2|\psi(r)|^4 \rangle_t = 3$.

increased only in the very narrow vicinity of the localization center.

Second, the DNLSM appears to describe the spatial structure of background intensity of ALS's adequately in the Q1D Anderson model. The agreement is good for all values of t studied here. This verifies the assumption that the semiclassical picture of a diffusive electron accounts for the origin of ALS's in the Q1D Anderson model.

Third, we must emphasize that at least in the Q1D case it appears to be difficult to reach the asymptotic regime where Eq. (9) is valid. We have thus not been able to observe the line shape suggested¹⁶ to be characteristic of ALS's in Q1D samples. We expect, however, that this characteristic shape is approached further as t is increased.

Fourth, fluctuations around the average ALS's, in Q1D, are consistent with Eq. (10). The agreement is the better the larger the t , as seen in Fig. 3. This is so because Eq. (10) was derived in Ref. 16 using asymptotic expressions.

Fifth, in 3D samples the fluctuations around the average ALS's appear to be consistent with RMT, although the second moment is somewhat larger than expected according to RMT.

Finally, we briefly consider the region $r < l$. In the 3D case, the central peak is found to be very narrow. It is possibly narrower than the electronic mean free path l , which is of the order of several lattice spacings in the metallic

regime.¹² This may indicate that the DNLSM is not applicable in this case, since l is the shortest relevant length scale in the DNLSM. It may also point towards the conjecture of Refs. 8 and 6 where high wave-function amplitudes were suggested to arise from partial trapping of electrons in rare local potential cavities. Such features are not included in the DNLSM. At this, point, however, we cannot offer quantitative results concerning the parametric dependence of the width of the central peak.

In conclusion, we have studied the spatial structure and statistics of anomalously localized states in the Anderson model. Our results indicate²⁰ that the spatial structure of ALS's in Q1D and 3D samples is very different, as surmised in Refs. 16, 8, and 6. Our results are consistent with the idea that the origin of ALS's is different in quasi-one-dimension Q1D and in three dimensions. In order to decide to which extent local potential traps are relevant in 3D, it would be of great interest to study the parametric dependence of the width of the local maximum seen in Fig. 2. In this context, a continuous model would probably be more suitable than the discrete lattice Hamiltonian (1) studied in the present paper.

This work was supported by a grant from the Swedish Science Council, by the DFG (SFB 393), and by the European Research Training Network QTRANS.

*On leave from Institut für Physik, Technische Universität, D-09107 Chemnitz, Germany.

¹P.W. Anderson, Phys. Rev. **109**, 1492 (1958).

²A.D. Mirlin and Y.V. Fyodorov, J. Phys. A **26**, L551 (1993).

³Y.V. Fyodorov and A.D. Mirlin, Int. J. Mod. Phys. B **8**, 3795 (1994).

⁴V.I. Fal'ko and K.B. Efetov, Phys. Rev. B **52**, 17 413 (1995).

⁵K.B. Efetov, Adv. Phys. **32**, 53 (1983).

⁶A.D. Mirlin, Phys. Rep. **326**, 259 (2000).

⁷K. Müller, B. Mehlis, F. Milde, and M. Schreiber, Phys. Rev. Lett. **78**, 215 (1997).

⁸I.E. Smolyarenko and B.L. Altshuler, Phys. Rev. B **55**, 10 451 (1997).

⁹Y.M. Blanter, A.D. Mirlin, and B.A. Muzykantskii, Phys. Rev. B **63**, 235315 (2001)

¹⁰V. Uski, B. Mehlis, and M. Schreiber, Phys. Rev. B **63**, 241101(R) (2001).

¹¹V. Uski, B. Mehlis, R.A. Römer, and M. Schreiber, Phys. Rev. B **62**, R7699 (2000).

¹²B.K. Nikolić, Phys. Rev. B **65**, 012201 (2002).

¹³In the paper by B.K. Nikolić and P.B. Allen, Phys. Rev. B **64**, 014203 (2001), the spatial structure of an ALS's is exemplified in Fig. 1 (top).

¹⁴A. Ossipov, T. Kottos, and T. Geisel, Phys. Rev. E **65**, 055209 (2002).

¹⁵In the strongly disordered regime, localization due to trapping in potential wells was discussed by E.N. Economou, C.M. Soukoulis, and A.D. Zdetsis, Phys. Rev. B **30**, 1686 (1984).

¹⁶A.D. Mirlin, J. Math. Phys. **38**, 1888 (1997).

¹⁷F. Haake, *Quantum Signatures of Chaos*, 2nd ed. (Springer, Berlin, 1992).

¹⁸M.L. Mehta, *Random Matrices* (Academic Press, Boston, 1990).

¹⁹U. Elsner *et al.*, SIAM J. Sci. Comput. (USA) **20**, 2089 (1999).

²⁰It cannot be excluded with certainty, however, that in the 3D case the most localized states are found only for some special configurations (Ref. 8) of the disorder potential which may not have appeared in the—necessarily finite—ensemble of samples analyzed here.

²¹Note the following misprint in Ref. 10: the labels $X=0.97$ and $X=0.79$ in Fig. 3 were erroneously interchanged.